Hindawi
International Journal of Polymer Science
Volume 2022, Article ID 9733138, 11 pages
https://doi.org/10.1155/2022/9733138

Research Article

Stress Dependency of Creep Response for Glass/Epoxy Composite at Nonlinear and Linear Viscoelastic Behavior

N. Nosrati[1], **A. Zabett**[1,2] **and S. Sahebian**[1]

[1]*Department of Materials Science and Engineering, Ferdowsi University of Mashhad, Mashhad, Iran*
[2]*Sun Air Research Institute, Ferdowsi University of Mashhad, Mashhad, Iran*

Correspondence should be addressed to S. Sahebian; s.sahebian@um.ac.ir

Received 27 July 2021; Revised 12 November 2021; Accepted 23 November 2021; Published 10 February 2022

Academic Editor: Atsushi Sudo

This research is aimed at comparing the stress dependency of creep viscoelastic behavior for glass/epoxy composite and neat epoxy close to the glass transition temperature and room temperature. Long-term creep performance of quasi-unidirectional composites and quasi-isotropic stacking sequence composites is modeled based on the time-stress superposition principle (TSSP). Linearity and nonlinearity of viscoelastic behavior and stress-dependence correlations were investigated for quasi-isotropic stacking sequence composite at 25°C and 50°C (near the glass transition temperature). Stress dependency of creep stages (primary, secondary, and tertiary) of neat epoxy was evaluated at this range of temperature. The prediction results of composite at room temperature show that the raising of the stress levels leads to the acceleration of viscoelastic strain values, but the creep compliance does not present any dependency. Besides, the reduction of viscoelastic ability is realized by measuring less amount of creep compliance at higher stress level in the glass transition temperature. These observations confirmed the linearity and nonlinearity of viscoelastic behavior at room and glass transition temperature, respectively. Similar results of neat epoxy revealed that the increase in the stress level accelerates the strain values at room temperature and decreases the creep resistance at glass transition temperature. Failure morphologies of epoxy sample fractured at room temperature are included scarp, cusp, and river line; however, close to the glass transition temperature, more expansive mirror zones appeared. Fiber architecture significantly affected the secondary stage regime by providing load-bearing ability. Thereby, creep rate reduction and enhancement of creep lifetime and creep resistance would be reported using unidirectional reinforcing in contrast to those of the multilayer sequence one.

1. Introduction

Epoxy has gained enormous attention to use as a matrix in fiber-reinforced polymer (FRP) composites, due to relatively high chemical resistance, low volatility, low shrinkage on curing, and relatively high specific strength and modulus [1]. Viscoelasticity of epoxy affects the residual stiffness [2] and fatigue life during dynamic loading [3]. High viscoelastic ability is often the primary requisite for reliable long-term structural applications [4]. The viscoelastic properties of polymeric materials can be evaluated using the creep tests [5].

At long-term creep loading, nonlinear viscoelastic response increased by adding modifiers to asphalt binder [6] and increasing the stress and temperature value [7]. The nonlinearity impacted the creep compliance and relaxation modulus [6]. Deformation of polymeric materials becomes more critical as the temperature reaches the glass transition temperature (T_g) [8]. Polymer softening near T_g is a significant problem to deteriorate viscoelastic resistance [9]. Viscoelastic characterization under the impact of elevated temperature and T_g throughout the creep tests has been performed on polymeric matrix composites (PMC) in previous researches.

Ahci and Talreja [7] studied creep-recovery test data for graphite fiber thermoset composite with T_g value higher than 700°C. The composite displayed noticeable creep in the fiber direction when the temperature approached the T_g value, and it showed a nonlinear viscoelastic behavior beyond threshold stress of 13 ksi at 700°C. Sayyidmousavi et al. [10] conducted creep tests on polyimide resin-based carbon fiber composite at 180, 220, and 270°C. Increased temperature resulted in softening and acceleration of the creep strain. Moreover, the nonlinearities were produced at elevated temperatures.

Durante et al. [11] studied the creep behavior of polylactic acid reinforced by woven hemp fabric. They showed the increment of creep compliance by rising temperature. Reviewed studies of Eftekhari and Fatemi [12] demonstrated the significant impact of elevated temperature on polymer chains' increased mobility. Also, creep strain and creep rate increased with increasing temperature because of higher macromolecular mobility in polymer chains.

Wang et al. [13] investigated the creep and recovery behaviors of polystyrene composites filled with chemically reduced graphene oxide. They found that the creep deformation and strain rate increase with elevating temperature. Lu et al. [14] studied the effect of temperature on the creep behavior of resin matrix and basalt fiber-reinforced polymer (BFRP) experimentally. They reported as temperature exceeded T_g, a remarkable increase in strain is observed. Reis et al. [15] investigated the creep behavior of epoxy matrix composite in glassy, glass transition, and elastomeric regions. They concluded the higher deformation as temperature increases.

There is sparse in evaluating the comparison of creep response between nonlinear and linear viscoelastic behavior by increasing stress levels on polymeric composites. For this purpose, the impact of stress on viscoelastic strain is investigated at a glassy state and glass transition temperature of E-glass/epoxy composite. The time-stress superposition principle is used to predict long-term creep performance at 25°C and 50°C. Linearity and nonlinearity of viscoelastic behavior are determined by plotting an isochronous curve. The effect of stress on creep response at the primary and secondary stage is indicated at glassy state and glass transition temperature of neat epoxy. Morphologies of creep fractured epoxy surfaces are obtained and show the viscoelastic ability at 25°C and 50°C creep-fractured samples by scanning electron microscopy (SEM).

2. Methodology

2.1. Materials. Resin epoxy Epolam 2040 and hardener Epolam 2047 were purchased from Axson Technologies Company. According to the company datasheet, Table 1 shows the viscosity and density properties of the epoxy resin and hardener at room temperature. Unidirectional (0°, 90°) and biaxial (±45°) E-glass fibers were supplied from STA Company. Volumetric density of E-glass fibers is 2.58 g/cm^3, and its mechanical properties including tensile modulus, tensile strength, and elongation are 40.68 (GPa), 919 (MPa), and 2.685 (%), respectively.

2.2. Sample Preparation. Resin and hardener were mixed by a weight ratio of 100 : 32 for 5 min, preparing neat epoxy samples and the composite matrix. After mixing, the mixture was poured in the given mold (with the dimensions of type I in ASTM D-638) to prepare neat epoxy samples. The curing procedure was in two stages at 25°C for 24 hours and at 70°C for 16 hours. A vacuum infusion process (VIP) was employed to fabricate the E-glass/epoxy composite. The glass fiber arrangements (in seven plies) were as follows: [0°] for quasi-unidirectional composite and [90, 0, ±45, 0, ±45, 0, 90] for quasi-isotropic stacking sequence composite. The curing steps were the same as the neat epoxy procedure. The quasi-isotropic stacking sequence composites and quasi-unidirectional composites were labeled as MD (multidirectional) and UD (unidirectional).

Table 1: Physical properties of resin and hardener.

Properties	Resin Epolam 2040	Hardener Epolam 2047
Viscosity at 25°C(MPa·s)	1100	10
Density at 25°C (g/cm^3) (ISO 1675:1985)	1.16	0.94

Table 2: Condition of creep tests on the MD and UD samples.

Code of sample	Temperature (°C)	Stress (MPa) Reference-*failure*	Test time
MD	25	**40**, 129, 216, 302, 345, *354*	3 hours
MD	50	**40**, 100, 195, 311, *324*	1 hour
UD	50	**40**, 108, 311, 400, *450*	1 hour
Epoxy	25	32, *53*	2.5 hours
Epoxy	50	18, *32*	4 hours

2.3. Material Characterization

2.3.1. Tensile Test. Tensile tests were conducted as per the requirements and proposed dimensions of ASTM D3039 [16] on composite and ASTM D638 [17] on epoxy with a Zwick universal testing machine Z250 to determine the sample's mechanical properties. Ten rectangular-shaped composite samples and five dog bone-shaped neat epoxy samples have been tested under loading rate of 2 mm/min and 5 mm/min, respectively.

2.3.2. Dynamic Mechanical Analysis. To certify polymeric samples for application involving a range of temperature, dynamic mechanical thermal analysis (DMTA) is the most widely used technique. It was performed in three-point bending mode as per ASTM D7028 [18] using a Triton Technology DMTA machine (Ltd.). Measurements were recorded in the temperature range of 21-120°C at a heating rate of 5°C/min and oscillation frequency at 1 Hz. Glass transition temperature was determined using the tan delta peak method. Dimensions of the samples for DMTA were $37 \times 10 \times 1.8$ mm^3.

Table 3: Mechanical properties of the UD and the MD composites and the epoxy specimens.

Specimen	Elongation at break (avg) (%)	Standard deviation (σ)	Ultimate strength (MPa) (avg)	Standard deviation (σ)	Elastic modulus (GPa) (avg)	Standard deviation (σ)
MD	0.026	3.74×10^{-4}	433	1.34	18.2	0.67
UD	0.051	2.94×10^{-3}	804	8.68	17.3	0.31
Epoxy	4.54	1.95×10^{-3}	71	1	3.02	0.11

2.3.3. Creep Measurements. To study the time-dependent deformation of composite and neat epoxy samples, creep measurements were carried out using a Santam universal testing machine STM-150. According to ASTM D2990 [19], the test requirements and proposed dimensions were in a tensile mode and force control. Dimensions of epoxy and glass/fiber composite were based on ASTM D-638 (type ı) (mentioned in ASTM D2990). The condition of creep tests is summarized in Table 2. The sample was placed in the grips with level arm in vertical position. The displacement of crosshead was controlled by encoder feedback, measurement using sensor, and with the displacement resolution of 0.1 μm. The ratio of this amount to the initial length determined the strain value.

2.3.4. Scanning Electron Microscopy. Creep fracture morphologies of epoxy were characterized by scanning electron microscopy (SEM) using an LEO-1450VP operating at 20 kV. Before evaluation, fractured surfaces were coated with gold powder for electron absorption. Provided images were in the magnification of 100x, 500x, 2500x, and 4000x.

3. Results and Discussion

3.1. Tensile Test. Results from a tensile test of MD, UD, and epoxy specimens are summarized in Table 3. Ultimate tensile strength and elongation at break of the UD composite are twice those of the MD composite. In comparison, the elastic modulus of both composites is almost similar. Epoxy has an elongation at break, 89 times figure for the UD composite. From the results, it can be concluded that there is a substantial improvement (1032%) in tensile strength, from neat epoxy to unidirectionally reinforced epoxy matrix, as the fibrous phase mostly governs it.

3.2. Dynamic Mechanical Analysis (DMA). The present investigation provides insights into the viscoelastic properties of glass/epoxy composite and neat epoxy. Storage modulus (E'), loss modulus (E''), and loss factor, that is, tan δ, of specimens in the temperature range of 21-120°C are shown in Figure 1. Storage modulus is indicative of the elastic modulus, and loss modulus represents the amount of energy dissipated during heating of a material. The ratio of E''/E' is known as the loss factor.

Figure 1(a) represents the storage modulus of specimens. Fiber reinforcing of epoxy matrix stiffens the neat epoxy. Thus, the storage modulus of neat epoxy shows a remarkable increase upon the addition of glass fiber. However, irrespective of fiber orientation type, there is a decrease in E' with increasing temperature due to the increased molecular motion of polymer chain with temperature [20]. As the specimen approaches T_g, E' falls rapidly due to the onset of glass transition behavior.

Figure 1(b) shows that the peak height is higher in glass fiber composites. The reason might be that the polymer's viscoelastic deformability at the filler interface and small energy has been dissipated [21]. The peak factor (tan δ) versus temperature curve (Figure 1(c)) can determine T_g of specimens, which have been presented in Figure 1(d). A slight decrease in T_g can be attributed to the fiber reinforcing when filler surfaces do not partially participate in cross-linking reaction [22].

3.3. Prediction of Long-Term Creep. It is impractical to conduct creep tests for the entire lifetime of materials and to extract durable response of creep behavior of glass/epoxy composite [23]. Accelerated methods are essential for reducing the time and most of them are based on the superposition principle [24]. Time-stress superposition principle (TSSP) allows to extend curves over time and predicts long-term deformability. Accordingly, the viscoelastic response at higher stress is identical to that at the lower stress in a long time [25]. TSSP is based on the Doolittle formula, in which viscosity is shown to be a function of free volume [26], and its application was early found by O'Shaughnessy [27] and Ferry and Stratton [28].

The linearity of viscoelastic behavior of short-term creep data is the first and most crucial requirement for utilizing the TSSP model [29]. Isochronous curves are presented in Figure 2 for UD and MD composites at 25°C and 50°C. R square value of the linear fits in each stress-strain diagram confirmed the viscoelastic behavior's linearity for exploiting TSSP.

Steps of generating master curve at 25°C and 40 MPa are as follows.

First, single-step short-term creep tests were conducted at isotherm and reference stress ranging to failure stress. Accordingly, at 25°C, creep tests were performed for 3 hours at stress levels of 40, 129, 216, 302, 345, and 354 MPa for 27 minutes. Creep-strain time data are illustrated in Figure 3(a). After that, unshifted creep strain curves appear on a logarithmic time scale in Figure 3(b). Creep curves were shifted horizontally and vertically through a sufficient coefficient to achieve accepted fit at each curve's end. Horizontal and vertical shift factors are proposed to shift curves in time and strain scale, respectively [24].

A smooth master curve with suitable overlapping is obtained during the numerical shifting technique,

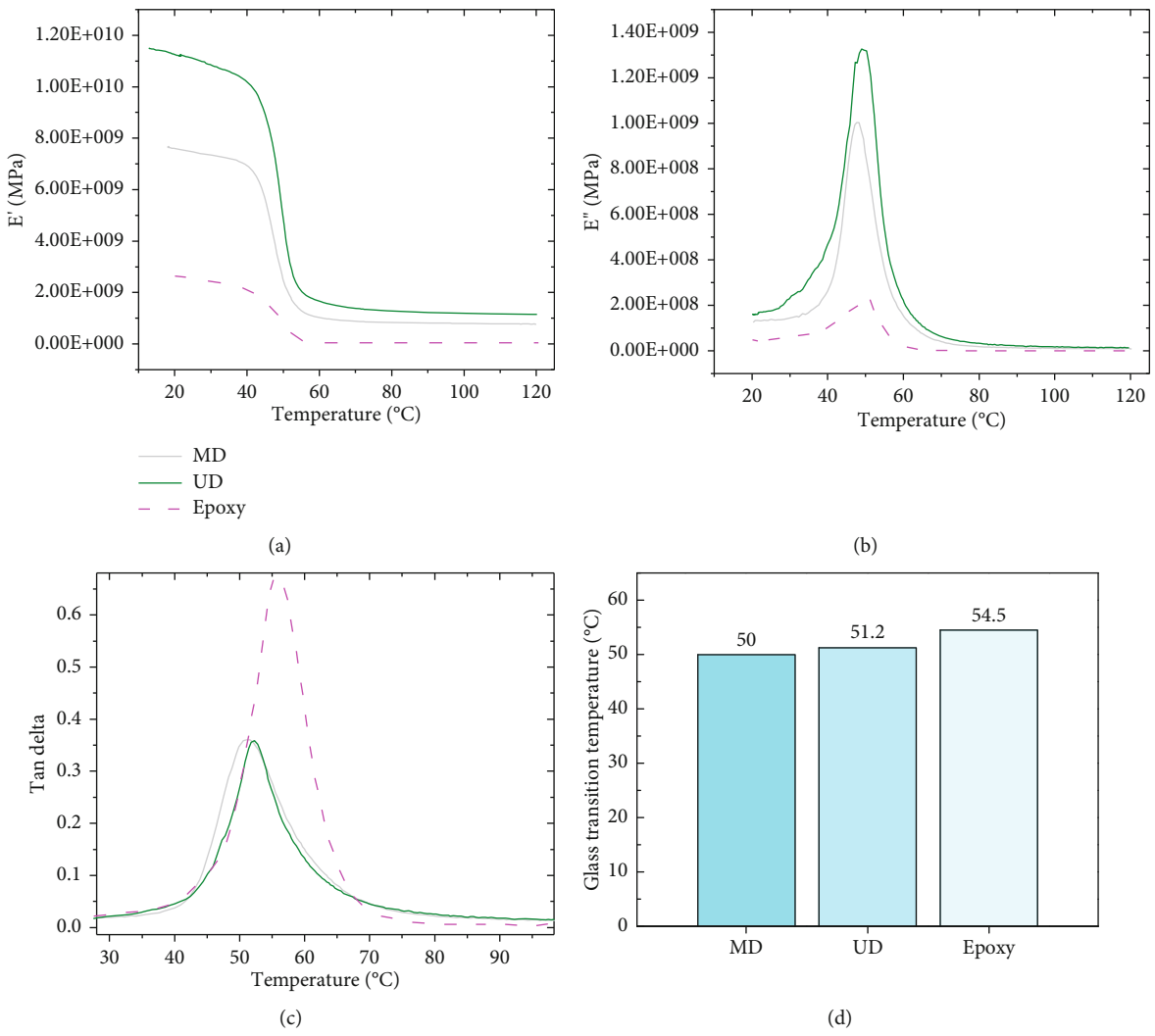

Figure 1: Line graphs of (a) the loss modulus, (b) the storage modulus, (c) the tan delta, and (d) the glass transition temperature for the UD and MD specimens.

represented in Figure 3(c). Numerical shifting technique (Rouleau, 2013), Arrhenius equation [23, 30], and manual shifting methods [9, 31] are exploited to generate long-term master curves. Finally, a schematic of the creep strain function of time is plotted in Figure 3(d). The long-term creep strain rate is estimated to be 6.1×10^{-14}, and the creep lifetime of MD composite is predicted to be 250 years (10^{10} s), approximately. The validity of this principle is confirmed as a proper matching of a theoretical master curve with the experimental tests [32, 33] and the curve simulated by the Findley power law [34].

3.4. Stress Dependency of Glass/Epoxy Composite. Figure 4 displays creep strain and creep compliance profiles of MD composite as a function of time, tested at 25°C and 50°C (near the glass transition temperature). The applied load was chosen within the elastic limit of the composite. Figure 4(a) shows the variation of compliance, defined by the ratio between the resulting strain and the applied stress, versus time at room temperature and different stress levels of 40, 129, and 216 MPa (10%, 30%, and 50% UTS, respectively). The relative coincidence of three compliance master curves represented the linearity of the long-term viscoelasticity at room temperature, and the compliance does not depend on stress levels. The other research mentioned this insight, the creep compliance at lower stress and temperature is independent on stress level, the volume expansion is limited, and so a linear behavior is observed [35].

As evident from Figure 4(b), creep strain increases rapidly with a rise in stress. For example at $t = 10^6$ s (277 hours), creep train increased by 50% (from 0.08 to 0.19%) and by 0.57% (from 0.19% to 0.30%), as the applied stress increased from 40 to 129 MPa and 129 MPa to 216 MPa, respectively. It could show the ability to accelerate strain by increasing stress at the linear viscoelastic region. Based on (a) $\eta = \sigma/\varepsilon_o$ [36], at the linear viscoelastic response and constant η, by increasing stress, ε_o must increase and according to this viscoelastic strain is accelerated.

The creep lifetime and strain rate are summarized in Table 4. It shows an increment of creep strain rate from 6.8×10^{-12} (s^{-1}) to 4.0×10^{-10} (s^{-1}) and the reduction of creep lifetime from six years and three months ($10^{8.3}$ s) to

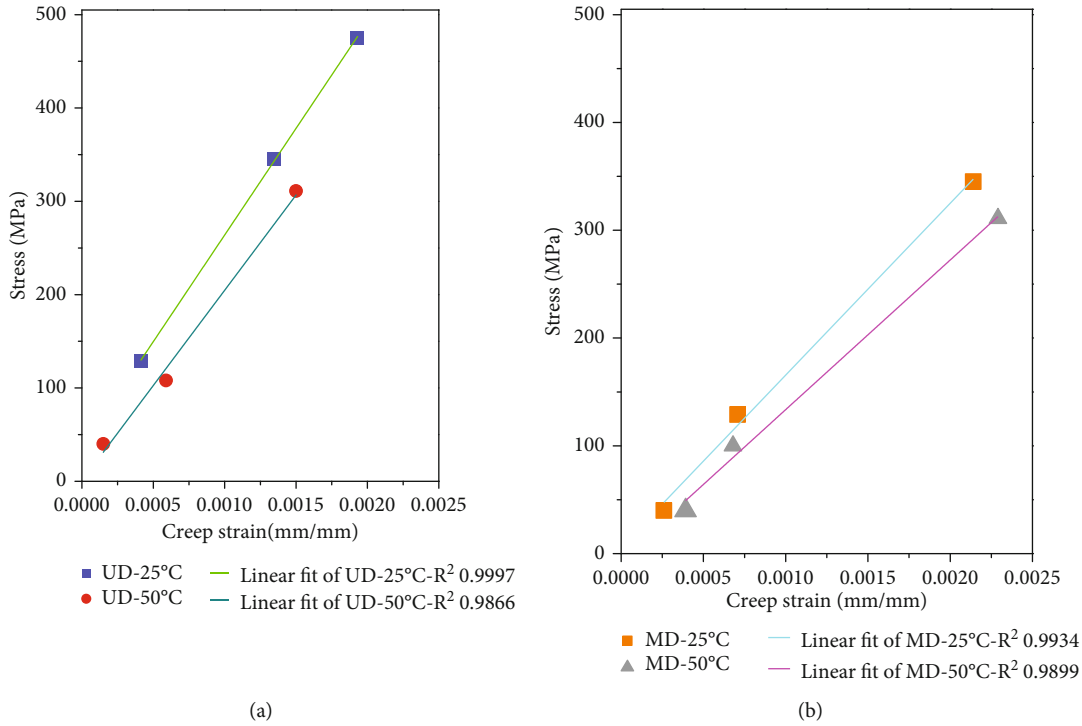

Figure 2: Isochronous curves at 25°C and 50°C for (a) the UD and (b) the MD composites.

16 days ($10^{6.14}$ s), on rising the stress level from 129 MPa to 216 MPa.

In the line graphs at Figure 4(c), the creep compliance at 10^8 (s) for stress levels of 40, 100, and 195 MPa (10%, 23%, and 45% UTS, respectively) is 136, 60, and 26 ($\times 10^{-12}$) Pa^{-1}. Because of the significant difference in compliance amount, it is concluded that the viscoelastic behavior is stress-dependent and nonlinear. The nonlinearity is derived from the stress-dependent time response in the deformation process [37]. As the nonlinearity achieved, the compliance is no longer independent on the stress levels and the creep phenomena are no longer reversible [35].

In Figure 4(d), at $t = 10^7$ s, by increasing stress from 40 to 195 MPa, viscoelastic strain reduces from 0.0030 to 0.0026. According to the relation (a) and Figure 4(c), by increasing stress levels, η rises and for this reason, creep strain may not be increased significantly. It could be concluded that an increase in stress level at the nonlinear region leads to a reduction in viscoelastic ability. Goertzen and Kessler [31] reported the creep resistance might reduce near the glass transition temperature. Such reduction might be ascribed to the fact that the increase in temperature will cause a reduction in the activation barrier for the dissociation of various interchain bonds, thus allowing the polymer to untangle, slip, and reorient quickly [38].

3.5. Stress Dependency of Epoxy. It is essential to consider the stress dependency of epoxy's viscoelastic behavior as a composite matrix at the glassy state and glass transition state. At room temperature, epoxy's creep behavior is evaluated at 32 and 53 MPa (see Figure 5(a)). In the line graph's primary stage, creep response at higher stress saw a lower strain value (0.002 mm/mm) at lower time 360 s than the figure for 32 MPa (0.0055 mm/mm and 1850 s) to complete strain hardening and to enter the transient stage.

In the transient stage, creep rate at a higher stress level (53 MPa) saw more amount than that of the 32 MPa. It is seen that increasing stress leads to accelerate strain, and it is realized that epoxy plays a linear viscoelastic response at this condition region. It could be due to faster polymer chain reorientation to damp higher energy applied on the epoxy system. Constant load for a prolonged period of creep might result in stretching and reorientation of polymer chains that are eventually leading to a failure [39].

At glass transition temperature, changes of stress have a considerable effect on creep curve format. For example, the graph for higher stress at the primary stage shows a longer time and strain to perform the strain-hardening mechanism. Viscoelastic strain and time at the endpoint of the primary stage are 0.0295 and 8846 s for 32 MPa and 0.012 and 3126 s for 18 MPa. Such expansion in the primary stage might result from weak energy bonds during glass transition as stress increases. This reduction of energy bond makes the polymer chain stretch for a higher amount of strain to harden the epoxy system. Several types of molecular motions, including flexible polymeric chains, may rearrange quickly on the repeating unit length scale above their T_g, and after a longer duration, the polymeric chains get disentangled [40].

It is seen a negligible region of the secondary stage at 32 MPa. Such shortened steady state could be a result of a reduction in viscoelastic ability at T_g. Increasing σ might lead to progress transition from glassy to rubbery state and deteriorate viscoelastic resistance of epoxy. For this reason,

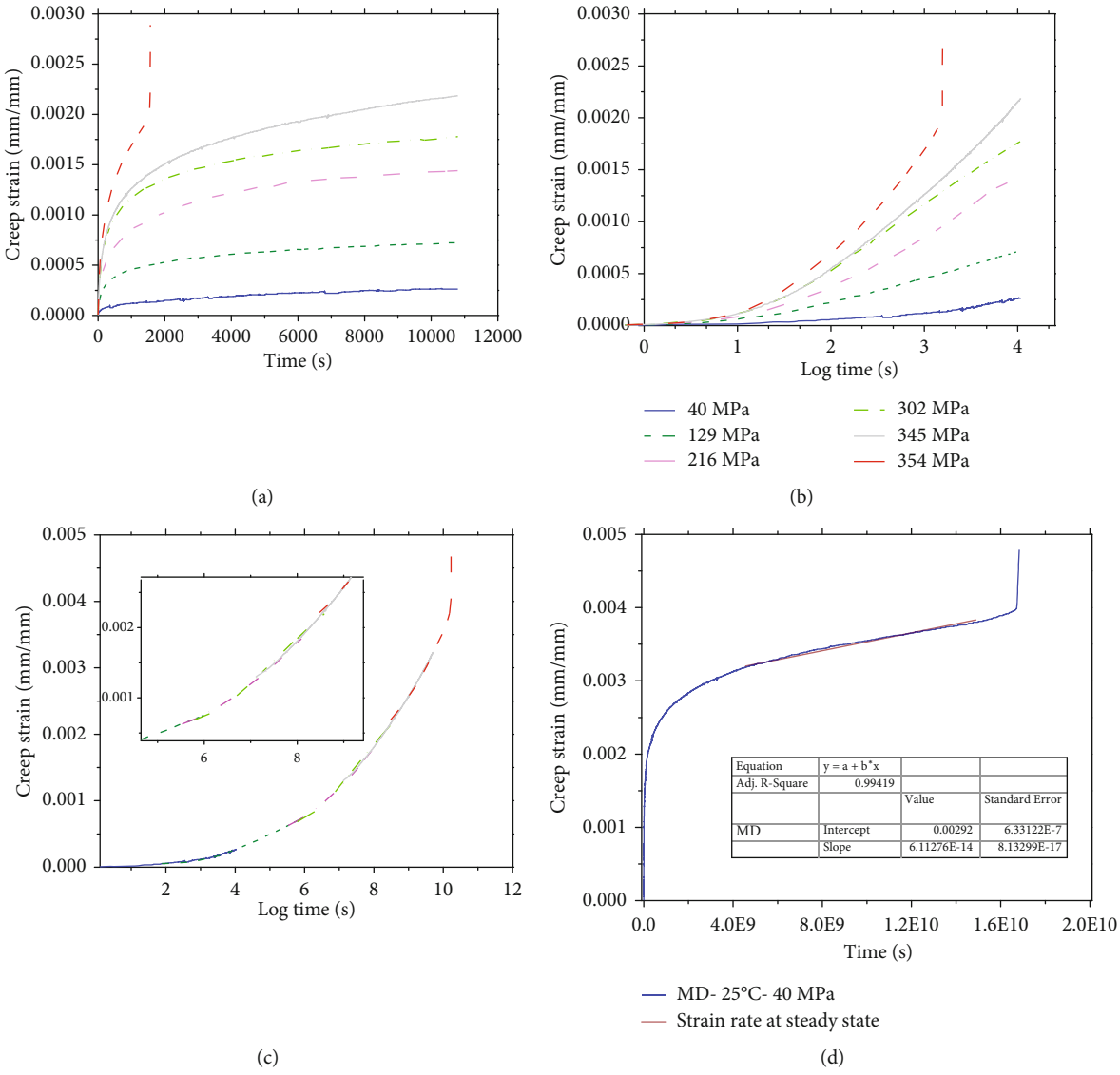

Figure 3: Sequences of generating master curve: (a) creep strain versus time, (b) creep strain versus logarithm of time, (c) shifted creep curves, and (d) master curve for the MD composite at 25°C and 40 MPa.

the nonlinearity of viscoelastic behavior could be indicated. As the other research reported, the transition between the linear and the nonlinear regime takes place more rapidly when the stress increases at higher temperature [35]. In general, viscous flow at high temperatures causes higher molecular chain relaxation and insufficient properties [41].

3.6. Scanning Electron Microscopy Analysis. Scanning electron microscopy was performed on creep-fractured epoxy samples to evaluate viscoelastic resistance at glassy and glass transition state. Fractographic images of the creep test at 25°C/53 MPa are shown in Figures 6 and 7. In Figure 6, the beginning of crack growth and layer separation initiated from a defect. By propagation of the crack, the mirror zone was created (smooth and glassy area). This region's size and width (subcritical crack growth) increase with time and temperature [42]. The transition region from mirror zone to rough zone was seen, and the rough zone was marked as a plastic deformation region by fine and little bigger three-dimensional epoxy.

In Figure 7(a), plastic deformation zone is observed, and in higher magnification, there are some cusps in Figure 7(b). Textured microflow was observed in most areas more than cusps formed partially in the plastic deformation zone. Other deformation mechanisms are included scarp and river line in Figures 7(c) and 7(d). Scarps located at the boundary between the crack planes and the river line are fractographic features for diagnosing crack growth directions. Scarp is most clearly seen in brittle matrix systems [43].

The failure mechanism typically changes at elevated temperatures as compared to ambient temperature. The fractographic analysis was performed on the epoxy sample fractured in a creep test at 50°C. In Figure 8(a), the dominant morphology was the mirror zone, and for this reason, the

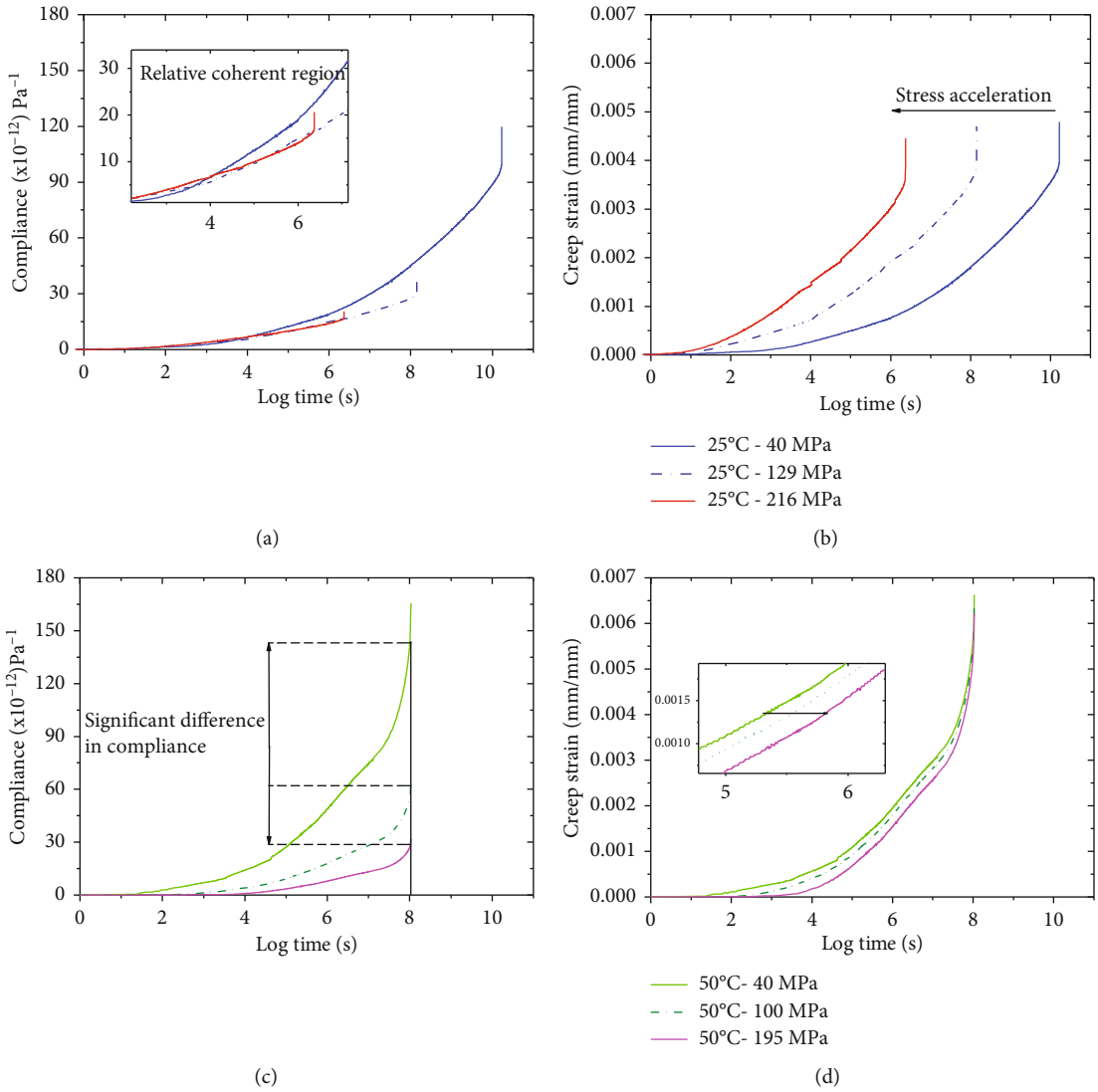

Figure 4: (a) Creep compliance and (b) creep strain master curves at 25°C and stress levels of 40, 129, and 216 MPa and (c) creep compliance and (d) creep strain master curves at 50°C and stress levels of 40, 100, and 195 MPa for the MD composite.

Table 4: The result of the master curve at different stress levels for the MD specimens at 25°C.

Stress (MPa)	Creep strain rate (s^{-1})	Creep lifetime
40	6.1×10^{-14}	250 years
129	6.8×10^{-12}	Six years and three months
216	4.0×10^{-10}	18 days

epoxy treats like semirubber polymer near T_g. Crack propagates from a defect and by making a rib reach to the next shear plane. The dimensions of the mirror zone increase rapidly by increasing temperature [42]. Figure 8(b) shows a relatively smooth surface containing some local plastic deformation as a continuous line on the mirror zone has been observed for neat epoxy. At higher magnification, scarps are detected as a local plastic deformation (Figure 8(c)).

3.7. Fiber Architecture Effect. Some fibers including carbon, glass, and aramid are applied to improve creep performance and polymer strength. However, composites tend to creep and soften which results in buckling and failure of load-carrying capabilities [44]. The stacking sequence had a distinct effect on the creep resistance depending on the region of glassy, glass transition, and rubbery states [45]. For this reason, fiber architecture impact is investigated on creep performance of the glass/epoxy composite near the glass transition temperature. Variation of creep strain and creep compliance in the function of time is illustrated in Figure 9 at 50°C and stress level of 40 MPa for the UD and the MD composites.

By contrast, in Figures 9(a) and 9(b), the primary stage in both composites has no visible difference, and it has the same regime. It could be due to the fact that epoxy matrix plays a prominent role at the primary stage and before transferring stress to fiber that epoxy molecular stretched. Hence,

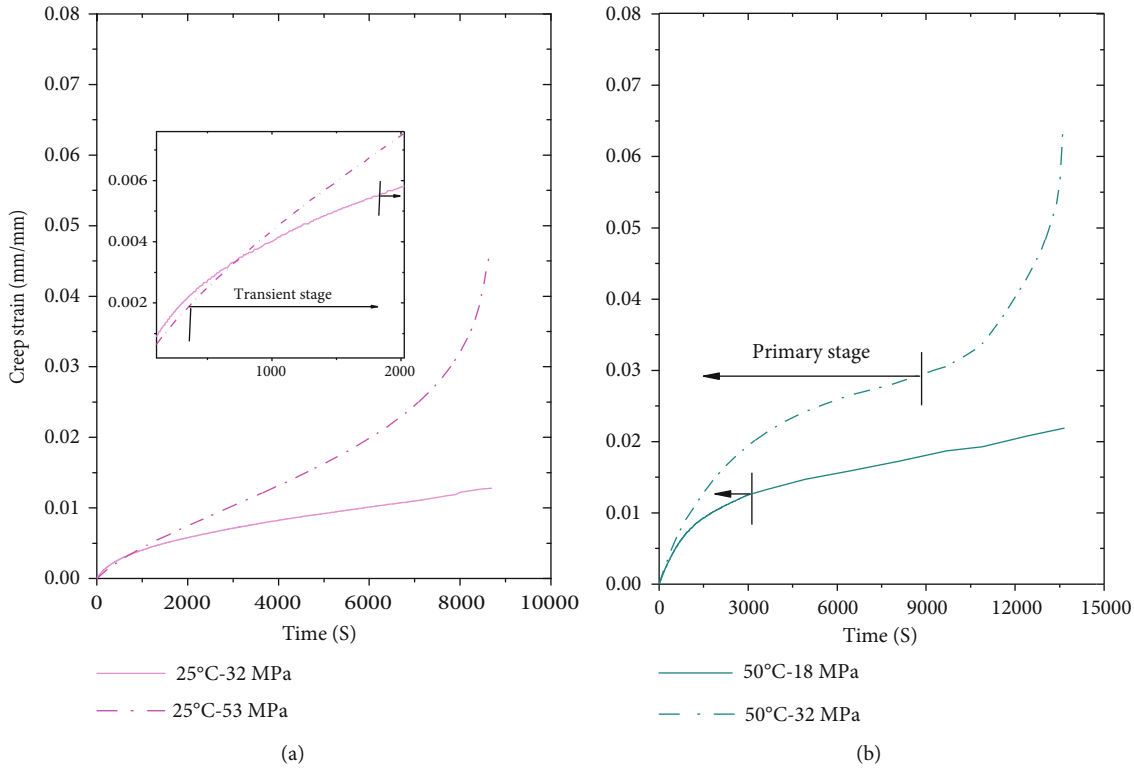

Figure 5: Schematic format of creep failure for neat epoxy (a) at room temperature (32 and 53 MPa) and (b) at the glass transition temperature (18 and 32 MPa).

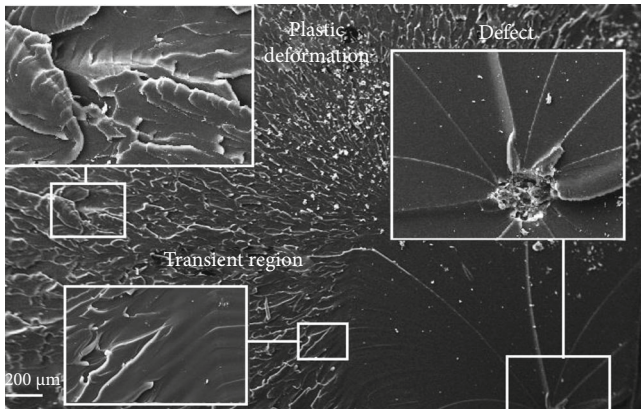

Figure 6: Micrograph image of epoxy sample fractured at 25°C creep test.

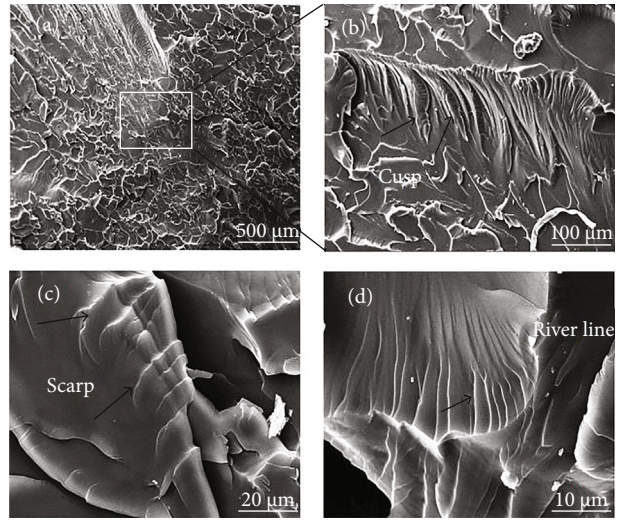

Figure 7: Micrograph images of epoxy sample fractured at 25°C creep test.

both composites display a similar profile at the primary stage because of the same matrix system.

By completing the stretch as the main mechanism at the primary stage, creep stress transfers from the matrix to the fiber. Since unidirectional fiber supports most of the pressure on the UD sample, less stress is sustained by epoxy, and therefore, the epoxy matrix is under lower stress than the MD sample. For this reason, creep rate at steady state saw lower slope value for UD composite. The creep strain rate is estimated to be 4.21×10^{-15} for the UD composite and 2.73×10^{-11} for the MD composite. It could be concluded that the mechanisms at the transient stage could depend on the stacking sequence in the similar temperature and stress level. Similarly, Li et al. [46] reported the creep strain rate of composite with 0° fiber angle is lower than that of the composites with 15°, 30°, and 45° fiber angle.

The creep lifetime of the UD composite is predicted 12,680 years ($10^{11.6}$ s), which is 4004 times that of the MD composite (three years and two months (10^8 s)). It is visible that the unidirectional composites have a significant potential to resist sudden failure near its T_g. It could be due to

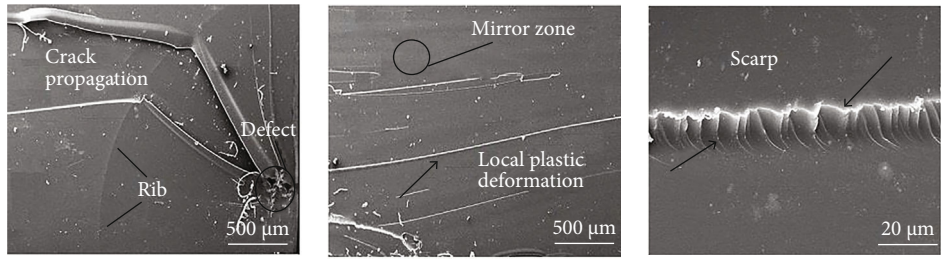

Figure 8: Micrograph image of epoxy sample fractured at 50°C creep test.

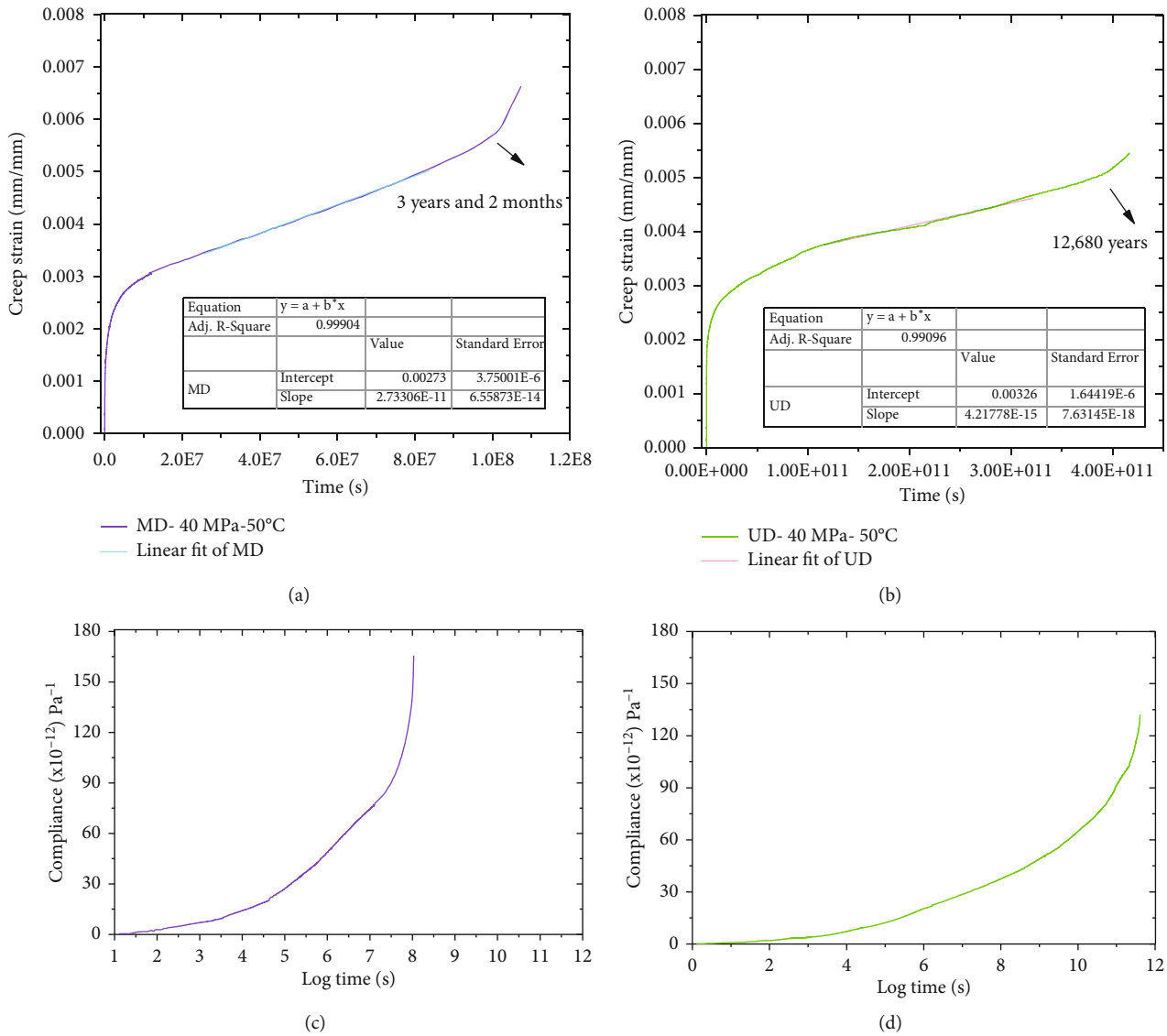

Figure 9: Stacking sequence effect on (a) creep strain and (c) compliance for the MD composites and the effect on the (b) creep strain and (d) compliance for the UD composites, near the glass transition temperature (50°C) and at 40 MPa.

the fact that the stress applied to the unidirectional composite is entirely supported by fibers [46].

In the comparison in Figures 9(c) and 9(d), compliance within 10^7 s (115 days) was determined to be 74×10^{-12} Pa^{-1} for the MD and decreased by 61% to the 29×10^{-12} Pa^{-1} for the UD composite. Such a reduction in creep compliance was also observed in higher percent at the breakpoint. It can mainly state that the creep behavior of the samples is strongly dependent on the fiber architecture. Almeida Jr. et al. found that the creep resistance

decreases from longitudinal to transversal fiber orientation [47].

4. Conclusion

The present study highlights new insights into the influence of stress on viscoelastic behavior at the linear and nonlinear region of polymeric materials. The main results are as follows:

(1) At the glassy state and the linear viscoelastic behavior of glass/epoxy composite, increased stress causes viscoelastic strain acceleration. However, nonlinear viscoelasticity near the glass transition temperature represented reduction in viscoelastic resistance and strain value as stress increases

(2) Creep compliance is independent on applied stress levels at room temperature that confirm the linearity of viscoelastic behavior, whereas near the glass transition temperature, the nonlinearity can be observed by compliance dependency on stress levels

Furthermore, the following are about the neat epoxy samples:

(3) The acceleration of the onset strain of the transient stage and the strain rate enhancement are observed at higher stress level and room temperature. In contrast, the exposure to the glass transition temperature provides negligible viscoelastic strain at the steady state and creates a sudden failure at the tertiary regime

(4) Fractography of the neat epoxy samples fractured at room temperature demonstrated plastic deformation morphologies included scarp, cusp, and river line that represented high resistance of viscoelasticity. Besides, by observing the mirror zone and partial plastic deformation at the glass transition temperature, the reduction in viscoelastic resistance could be concluded

Finally, the significant impact of fiber architecture on creep resistance is indicated on secondary stage due to the different loading support of fiber that could change the sustained stress by epoxy matrix. Quasi-unidirectional composite shows higher viscoelastic resistance because of the longer creep lifetime and lower creep rate value.

Data Availability

The authors confirm that the data supporting the findings of this study are available within the article.

Conflicts of Interest

The authors declare that they have no conflict of interest.

References

[1] A. E. Krauklis, A. G. Akulichev, A. I. Gagani, and A. T. Echtermeyer, "Time–temperature–plasticization superposition principle: predicting creep of a plasticized epoxy," *Polymers*, vol. 11, no. 11, p. 1848, 2019.

[2] S. S. Samareh-Mousavi and F. Taheri-Behrooz, "A novel creep-fatigue stiffness degradation model for composite materials," *Composite Structures*, vol. 237, article 111955, 2020.

[3] A. V. Movahedi-Rad, T. Keller, and A. P. Vassilopoulos, "Creep effects on tension-tension fatigue behavior of angle-ply GFRP composite laminates," *International Journal of Fatigue*, vol. 123, pp. 144–156, 2019.

[4] S. Kumar Ghosh, R. K. Prusty, D. K. Rathore, and B. C. Ray, "Creep behaviour of graphite oxide nanoplates embedded glass fiber/epoxy composites: emphasizing the role of temperature and stress," *Composites Part A: Applied Science and Manufacturing*, vol. 102, pp. 166–177, 2017.

[5] K. Deshmukh, T. Kovářík, A. Muzaffar, M. B. Ahamed, and S. K. Pasha, "Mechanical analysis of polymers," in *Polymer Science and Innovative Applications*, pp. 117–152, Elsevier, 2020.

[6] P. Hajikarimi, F. Moghadas Nejad, A. Khodaii, and E. H. Fini, "Introducing a stress-dependent fractional nonlinear viscoelastic model for modified asphalt binders," *Construction and Building Materials*, vol. 183, pp. 102–113, 2018.

[7] E. Ahci and R. Talreja, "Characterization of viscoelasticity and damage in high temperature polymer matrix composites," *Composites Science and Technology*, vol. 66, no. 14, pp. 2506–2519, 2006.

[8] Y. C. Ching, T. U. Gunathilake, K. Y. Ching et al., "Effects of high temperature and ultraviolet radiation on polymer composites," in *Durability and Life Prediction in Biocomposites, Fibre-Reinforced Composites and Hybrid Composites*, pp. 407–426, Elsevier, 2019.

[9] A. O. Fulmali, B. Sen, B. C. Ray, and R. K. Prusty, "Effects of carbon nanotube/polymer interfacial bonding on the long-term creep performance of nanophased glass fiber/epoxy composites," *Polymer Composites*, vol. 41, no. 2, pp. 478–493, 2020.

[10] A. Sayyidmousavi, H. Bougherara, I. el Sawi, and Z. Fawaz, "Investigation of the viscoelastic response of high temperature AS4-12K/RP46 composites using a micromechanical approach," *Polymer Composites*, vol. 37, no. 5, pp. 1407–1414, 2016.

[11] M. Durante, A. Formisano, L. Boccarusso, A. Langella, and L. Carrino, "Creep behaviour of polylactic acid reinforced by woven hemp fabric," *Composites Part B: Engineering*, vol. 124, pp. 16–22, 2017.

[12] M. Eftekhari and A. Fatemi, "Tensile, creep and fatigue behaviours of short fibre reinforced polymer composites at elevated temperatures: a literature survey," *Fatigue & Fracture of Engineering Materials & Structures*, vol. 38, no. 12, pp. 1395–1418, 2015.

[13] X. Wang, L. X. Gong, L. C. Tang et al., "Temperature dependence of creep and recovery behaviors of polymer composites filled with chemically reduced graphene oxide," *Composites Part A: Applied Science and Manufacturing*, vol. 69, pp. 288–298, 2015.

[14] Z. Lu, G. Xian, and K. Rashid, "Creep behavior of resin matrix and basalt fiber reinforced polymer (BFRP) plate at elevated temperatures," *Journal of Composites Science*, vol. 1, no. 1, p. 3, 2017.

[15] A. K. D. Reis, F. M. Monticelli, R. M. Neves, L. F. de Paula Santos, E. C. Botelho, and H. Luiz Ornaghi Jr., "Creep behavior of polyetherimide semipreg and epoxy prepreg composites: structure vs. property relationship," *Journal of Composite Materials*, vol. 54, no. 27, pp. 4121–4131, 2020.

[16] Testing, American Society for, and Materials, *Standard Test Method for Tensile Properties of Polymer Matrix Composite Materials*, ASTM international, 2006.

[17] Plastics, ASTM Committee D-20, *Standard Test Method for Tensile Properties of Plastics*, ASTM International, 2010.

[18] ASTM–D, *Standard Test Method for Glass Transition Temperature (DMA T_g) of Polymer Matrix Composites by Dynamic Mechanical Analysis (DMA)*, ASTM International, West Conshohocken, PA, 2007.

[19] ASTM, D, *2990-01. Standard Test Methods for Tensile, Compressive, and Flexural Creep and Creep-Rupture of Plastics*, ASTM International, West Conshohocken, 2001.

[20] J. S. Shelley, P. T. Mather, and K. L. DeVries, "Reinforcement and environmental degradation of nylon-6/clay nanocomposites," *Polymer*, vol. 42, no. 13, pp. 5849–5858, 2001.

[21] S. G. Prolongo, M. R. Gude, and A. Ureña, "Improving the flexural and thermomechanical properties of amino-functionalized carbon nanotube/epoxy composites by using a pre-curing treatment," *Composites Science and Technology*, vol. 71, no. 5, pp. 765–771, 2011.

[22] G. Tsagaropoulos and A. Eisenberg, "Dynamic mechanical study of the factors affecting the two glass transition behavior of filled polymers. Similarities and differences with random ionomers," *Macromolecules*, vol. 28, no. 18, pp. 6067–6077, 1995.

[23] S. K. Ghosh, P. Rajesh, B. Srikavya, D. K. Rathore, R. K. Prusty, and B. C. Ray, "Creep behaviour prediction of multi-layer graphene embedded glass fiber/epoxy composites using time-temperature superposition principle," *Composites Part A: Applied Science and Manufacturing*, vol. 107, pp. 507–518, 2018.

[24] J. Tanks, K. Rader, S. Sharp, and T. Sakai, "Accelerated creep and creep-rupture testing of transverse unidirectional carbon/epoxy lamina based on the stepped isostress method," *Composite Structures*, vol. 159, pp. 455–462, 2017.

[25] T. Glaskova-Kuzmina, A. Aniskevich, M. Zarrelli, A. Martone, and M. Giordano, "Effect of filler on the creep characteristics of epoxy and epoxy-based CFRPs containing multi-walled carbon nanotubes," *Composites Science and Technology*, vol. 100, pp. 198–203, 2014.

[26] A. K. Doolittle, "Studies in Newtonian flow. II. The dependence of the viscosity of liquids on free-space," *Journal of Applied Physics*, vol. 22, no. 12, pp. 1471–1475, 1951.

[27] M. T. O'Shaughnessy, "An experimental study of the creep of rayon," *Textile Research Journal*, vol. 18, no. 5, pp. 263–280, 1948.

[28] J. D. Ferry and R. A. Stratton, "The free volume interpretation of the dependence of viscosities and viscoelastic relaxation times on concentration, pressure, and tensile strain," *Kolloid Zeitschrift*, vol. 171, no. 2, pp. 107–111, 1960.

[29] J. Wang, X. Wang, Q. He, Y. Zhang, and T. Zhan, "Time-temperature-stress equivalence in compressive creep response of Chinese fir at high-temperature range," *Construction and Building Materials*, vol. 235, article 117809, 2020.

[30] N. Nosrati, A. Zabett, and S. Sahebian, "Long-term creep behaviour of E-glass/epoxy composite: time-temperature superposition principle," *Plastics, Rubber and Composites*, vol. 49, no. 6, pp. 254–262, 2020.

[31] W. K. Goertzen and M. R. Kessler, "Creep behavior of carbon fiber/epoxy matrix composites," *Materials Science and Engineering A*, vol. 421, no. 1-2, pp. 217–225, 2006.

[32] S. Loni, I. Stefanou, and J.-F. Caron, "On the application of the time-temperature-stress superposition principle (TTSSP) for the characterization of the creep behavior of glass fiber reinforced polymers (GFRP)," *JNC*, vol. 18, p. 2014, 2014.

[33] C. Wang, W. Luo, X. Liu, X. Chen, L. Jiang, and S. Yang, "Application of time-temperature-stress equivalence to nonlinear creep in poly(methyl methacrylate)," *Materials Today Communications*, vol. 21, article 100710, 2019.

[34] A. Amiri, N. Hosseini, and C. A. Ulven, "Long-term creep behavior of flax/vinyl ester composites using time-temperature superposition principle," *Journal of Renewable Materials*, vol. 3, no. 3, pp. 224–233, 2015.

[35] J. C. Qiao, J. M. Pelletier, and Y. Yao, "Creep in bulk metallic glasses. Transition from linear to non linear regime," *Materials Science and Engineering A*, vol. 743, pp. 185–189, 2019.

[36] K. P. Menard, *Dynamic Mechanical Analysis: A Practical Introduction*, CRC press, 2008.

[37] W. G. Knauss and I. J. Emri, "Nonlinear viscoelasticity based on free volume consideration," in *Computational Methods in Nonlinear Structural and Solid Mechanics*, pp. 123–128, Elsevier, 1981.

[38] M. Ganß, B. K. Satapathy, M. Thunga, R. Weidisch, P. Pötschke, and A. Janke, "Temperature dependence of creep behavior of PP–MWNT nanocomposites," *Macromolecular Rapid Communications*, vol. 28, no. 16, pp. 1624–1633, 2007.

[39] W. Zhang, A. Joshi, Z. Wang, R. S. Kane, and N. Koratkar, "Creep mitigation in composites using carbon nanotube additives," *Nanotechnology*, vol. 18, no. 18, article 185703, 2007.

[40] M. L. Cerrada, *Introduction to the Viscoelastic Response in Polymers*, 2005.

[41] N. P. Lorandi, M. O. H. Cioffi, C. Shigue, and H. L. Ornaghi Jr, "On the creep behavior of carbon/epoxy non-crimp fabric composites," *Materials Research*, vol. 21, no. 3, 2018.

[42] W. J. Cantwell, A. C. Roulin-Moloney, and T. Kaiser, "Fractography of unfilled and particulate-filled epoxy resins," *Journal of Materials Science*, vol. 23, no. 5, pp. 1615–1631, 1988.

[43] E. Greenhalgh, *Failure Analysis and Fractography of Polymer Composites*, Elsevier, 2009.

[44] H. Jena, J. K. Katiyar, and A. Patnaik, *Tribology of Polymer and Polymer Composites for Industry 4.0*, Springer, 2021.

[45] H. L. Ornaghi Jr., F. M. Monticeli, R. M. Neves, A. J. Zattera, M. O. H. Cioffi, and H. J. C. Voorwald, "Effect of stacking sequence and porosity on creep behavior of glass/epoxy and carbon/epoxy hybrid laminate composites," *Composites Communications*, vol. 19, pp. 210–219, 2020.

[46] Y. L. Li, W. J. Chen, M. Y. Shen, C. L. Chiang, and M. C. Yip, "Study on the mechanical properties and creep behaviour of carbon fiber nano-composites," in *Advanced Materials Research*, vol. 284, pp. 557–564, Trans Tech Publ, 2011.

[47] J. H. S. Almeida Jr., H. L. Ornaghi Jr., N. P. Lorandi, B. P. Bregolin, and S. C. Amico, "Creep and interfacial behavior of carbon fiber reinforced epoxy filament wound laminates," *Polymer Composites*, vol. 39, no. S4, pp. E2199–E2206, 2018.